

AD-A061 034

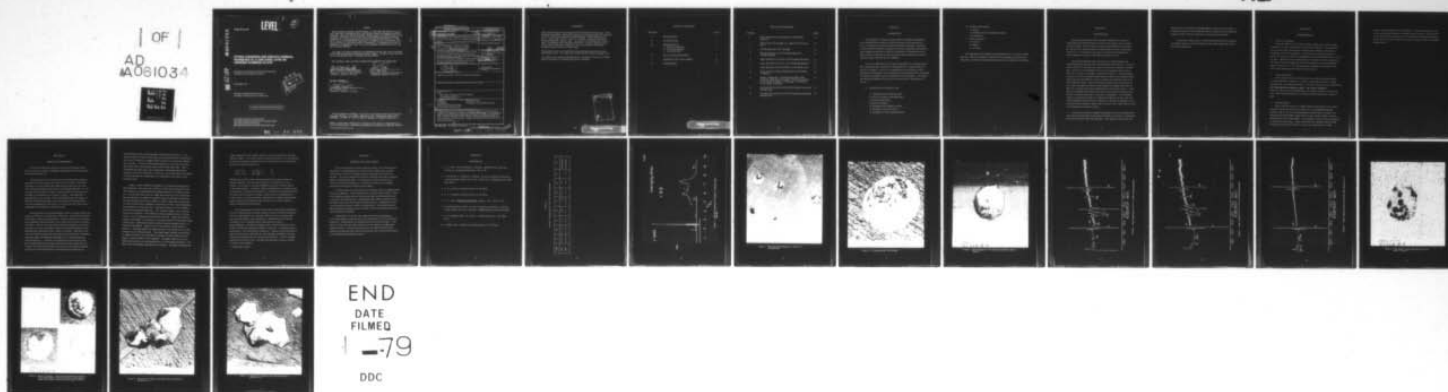
AIR FORCE MATERIALS LAB WRIGHT-PATTERSON AFB OHIO
PITTING CORROSION AND SURFACE CHEMICAL PROPERTIES OF A THIN OXI--ETC(U)
SEP 78 N T MCDEVITT, W L BAUN, J S SOLOMON
AFML-TR-78-128

F/G 11/6

UNCLASSIFIED

NL

OF
AD
A061034



AD A061034

DDC FILE COPY

AFML-TR-78-128

LEVEL

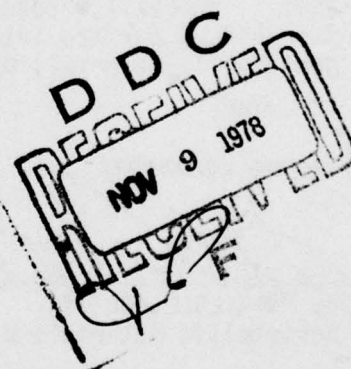
2
N.W.

**PITTING CORROSION AND SURFACE CHEMICAL
PROPERTIES OF A THIN OXIDE LAYER ON
ANODIZED ALUMINUM ALLOYS**

*MECHANICS AND SURFACE INTERACTIONS BRANCH
NONMETALLIC MATERIALS DIVISION*

SEPTEMBER 1978

TECHNICAL REPORT AFML-TR-78-128
Final Report for Period June 1977 to May 1978



Approved for public release; distribution unlimited.

AIR FORCE MATERIALS LABORATORY
AIR FORCE WRIGHT AERONAUTICAL LABORATORIES
AIR FORCE SYSTEMS COMMAND
WRIGHT-PATTERSON AIR FORCE BASE, OHIO 45433

78 11 06 090

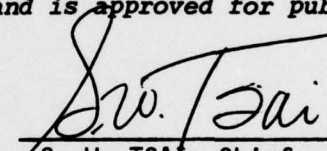
NOTICE

When Government drawings, specifications, or other data are used for any purpose other than in connection with a definitely related Government procurement operation, the United States Government thereby incurs no responsibility nor any obligation whatsoever; and the fact that the government may have formulated, furnished, or in any way supplied the said drawings, specifications, or other data, is not to be regarded by implication or otherwise as in any manner licensing the holder or any other person or corporation, or conveying any rights or permission to manufacture, use, or sell any patented invention that may in any way be related thereto.

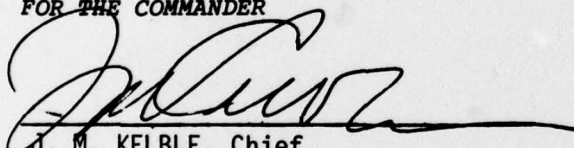
This report has been reviewed by the Information Office (OI) and is releasable to the National Technical Information Service (NTIS). At NTIS, it will be available to the general public, including foreign nations.

This technical report has been reviewed and is approved for publication.


NEIL T. McDEVITT, Project Engineer
Mechanics & Surface Interactions Br.
Nonmetallic Materials Division


S. W. TSAI, Chief
Mechanics & Surface Interactions Br.
Nonmetallic Materials Division

FOR THE COMMANDER


J. M. KELBLE, Chief
Nonmetallic Materials Division

"If your address has changed, if you wish to be removed from our mailing list, or if the addressee is no longer employed by your organization please notify AFML/MBM, W-PAFB, OH 45433 to help us maintain a current mailing list".

Copies of this report should not be returned unless return is required by security considerations, contractual obligations, or notice on a specific document.

SECURITY CLASSIFICATION OF THIS PAGE (When Data Entered)

DD FORM 1473
1 JAN 73

EDITION OF 1 NOV 65 IS OBSOLETE

UNCLASSIFIED

SECURITY CLASSIFICATION OF THIS PAGE (When Data Entered)

012328 11 06 090

FOREWORD

This technical report was prepared by Neil McDevitt and William L. Baun, Mechanics and Surface Interactions Branch, Nonmetallic Materials Division, Air Force Materials Laboratory (AFML/MBM), Wright-Patterson Air Force Base, Ohio, and Mr. James S. Solomon, University of Dayton Research Institute, Dayton, Ohio. The work was initiated under Project 2419, "Nonmetallic and Composite Materials", and was administered by the Air Force Materials Laboratory, Air Force Systems Command, Wright-Patterson Air Force Base, Ohio.

This report covers work conducted inhouse during the period June 1977 through May 1978. The report was released by the author in August 1978.

The authors are especially grateful to Mr. Brewster Stroop for his helpful advice and efforts in obtaining the SEM micrographs.

ACCESSION for
NTIS
DDC
ANNOUNCED
White Section ☒
F ☐
1954-1955
1956-1957
1958-1959
1960-1961
1962-1963
1964-1965
1966-1967
1968-1969
1970-1971
1972-1973
1974-1975
1976-1977
1978-1979
1980-1981
1982-1983
1984-1985
1986-1987
1988-1989
1990-1991
1992-1993
1994-1995
1996-1997
1998-1999
2000-2001
2002-2003
2004-2005
2006-2007
2008-2009
2010-2011
2012-2013
2014-2015
2016-2017
2018-2019
2020-2021
2022-2023
2024-2025
2026-2027
2028-2029
2030-2031
2032-2033
2034-2035
2036-2037
2038-2039
2040-2041
2042-2043
2044-2045
2046-2047
2048-2049
2050-2051
2052-2053
2054-2055
2056-2057
2058-2059
2060-2061
2062-2063
2064-2065
2066-2067
2068-2069
2070-2071
2072-2073
2074-2075
2076-2077
2078-2079
2080-2081
2082-2083
2084-2085
2086-2087
2088-2089
2090-2091
2092-2093
2094-2095
2096-2097
2098-2099
2100-2101
2102-2103
2104-2105
2106-2107
2108-2109
2110-2111
2112-2113
2114-2115
2116-2117
2118-2119
2120-2121
2122-2123
2124-2125
2126-2127
2128-2129
2130-2131
2132-2133
2134-2135
2136-2137
2138-2139
2140-2141
2142-2143
2144-2145
2146-2147
2148-2149
2150-2151
2152-2153
2154-2155
2156-2157
2158-2159
2160-2161
2162-2163
2164-2165
2166-2167
2168-2169
2170-2171
2172-2173
2174-2175
2176-2177
2178-2179
2180-2181
2182-2183
2184-2185
2186-2187
2188-2189
2190-2191
2192-2193
2194-2195
2196-2197
2198-2199
2200-2201
2202-2203
2204-2205
2206-2207
2208-2209
2210-2211
2212-2213
2214-2215
2216-2217
2218-2219
2220-2221
2222-2223
2224-2225
2226-2227
2228-2229
2230-2231
2232-2233
2234-2235
2236-2237
2238-2239
2240-2241
2242-2243
2244-2245
2246-2247
2248-2249
2250-2251
2252-2253
2254-2255
2256-2257
2258-2259
2260-2261
2262-2263
2264-2265
2266-2267
2268-2269
2270-2271
2272-2273
2274-2275
2276-2277
2278-2279
2280-2281
2282-2283
2284-2285
2286-2287
2288-2289
2290-2291
2292-2293
2294-2295
2296-2297
2298-2299
2300-2301
2302-2303
2304-2305
2306-2307
2308-2309
2310-2311
2312-2313
2314-2315
2316-2317
2318-2319
2320-2321
2322-2323
2324-2325
2326-2327
2328-2329
2330-2331
2332-2333
2334-2335
2336-2337
2338-2339
2340-2341
2342-2343
2344-2345
2346-2347
2348-2349
2350-2351
2352-2353
2354-2355
2356-2357
2358-2359
2360-2361
2362-2363
2364-2365
2366-2367
2368-2369
2370-2371
2372-2373
2374-2375
2376-2377
2378-2379
2380-2381
2382-2383
2384-2385
2386-2387
2388-2389
2390-2391
2392-2393
2394-2395
2396-2397
2398-2399
2400-2401
2402-2403
2404-2405
2406-2407
2408-2409
2410-2411
2412-2413
2414-2415
2416-2417
2418-2419
2420-2421
2422-2423
2424-2425
2426-2427
2428-2429
2430-2431
2432-2433
2434-2435
2436-2437
2438-2439
2440-2441
2442-2443
2444-2445
2446-2447
2448-2449
2450-2451
2452-2453
2454-2455
2456-2457
2458-2459
2460-2461
2462-2463
2464-2465
2466-2467
2468-2469
2470-2471
2472-2473
2474-2475
2476-2477
2478-2479
2480-2481
2482-2483
2484-2485
2486-2487
2488-2489
2490-2491
2492-2493
2494-2495
2496-2497
2498-2499
2500-2501
2502-2503
2504-2505
2506-2507
2508-2509
2510-2511
2512-2513
2514-2515
2516-2517
2518-2519
2520-2521
2522-2523
2524-2525
2526-2527
2528-2529
2530-2531
2532-2533
2534-2535
2536-2537
2538-2539
2540-2541
2542-2543
2544-2545
2546-2547
2548-2549
2550-2551
2552-2553
2554-2555
2556-2557
2558-2559
2560-2561
2562-2563
2564-2565
2566-2567
2568-2569
2570-2571
2572-2573
2574-2575
2576-2577
2578-2579
2580-2581
2582-2583
2584-2585
2586-2587
2588-2589
2590-2591
2592-2593
2594-2595
2596-2597
2598-2599
2600-2601
2602-2603
2604-2605
2606-2607
2608-2609
2610-2611
2612-2613
2614-2615
2616-2617
2618-2619
2620-2621
2622-2623
2624-2625
2626-2627
2628-2629
2630-2631
2632-2633
2634-2635
2636-2637
2638-2639
2640-2641
2642-2643
2644-2645
2646-2647
2648-2649
2650-2651
2652-2653
2654-2655
2656-2657
2658-2659
2660-2661
2662-2663
2664-2665
2666-2667
2668-2669
2670-2671
2672-2673
2674-2675
2676-2677
2678-2679
2680-2681
2682-2683
2684-2685
2686-2687
2688-2689
2690-2

TABLE OF CONTENTS

SECTION		PAGE
I	BACKGROUND	1
II	INTRODUCTION	3
III	EXPERIMENTAL	5
	1. Surface Preparation	
	2. Corrosion Solution	
	3. Instrumentation	
IV	RESULTS AND DISCUSSION	7
V	SUMMARY AND CONCLUSIONS	10
VI	REFERENCES	11

RESEARCH PAGE NOT FILMED
BLANK

LIST OF ILLUSTRATIONS

FIGURE		PAGE
1	SIMS-ISS Spectrum of Phosphoric Anodized 2024 Specimen	13
2	SEM Electron Micrograph of a Typical Pit Corrosion Area	14
3	Pit Showing Oxide Film Coverage	15
4	SEM Micrograph of a Pit Containing Spherical Growth Products	16
5	Auger Spectrum of a Pit on a 2024 Aluminum Specimen	17
6	Auger Spectrum of a Pit on a 7075 Aluminum Specimen	18
7	Auger Spectrum from the Surface Area Outside a Pit	19
8	X-Ray Image of Copper Obtained from the Pit Shown in Figure 4	20
9	Mosaic of SEM Data. Starting Upper Right Going Clockwise; SEM Electron Image of 7075 Pit Formation, X-Ray Image of Copper, X-Ray Image of Aluminum, X-Ray Image of Chlorine	21
10	Corrosion Pit Formed on Clad 2024 Showing Preferential Etching of Pit	22
11	Corrosion Pit Formed on Clad 7075 Showing Preferential Etching of Pit	23

SECTION I

BACKGROUND

The importance of metal-to-metal adhesive bonding technology has been established for secondary structural members of present day aircraft. Continued interest in this type of fabrication has led to a program to utilize bonded materials as primary structural components of airframes. This emphasis on primary structures necessitates a continuing research effort in this overall area in order to improve the life expectancy of these materials under real life service conditions.

In order to determine the average life expectancy of a bonded component, the present day researcher is confronted with a complex number of factors to consider. Factors to be considered cross a number of interdisciplinary technologies: (1) all components of the adhesive joint, (2) dynamic environment evaluation, and (3) mechanics of failure analysis. We propose the following breakdown of the above areas into specific study efforts as follows:

A. Components of the Adhesive Joint

- 1) metallurgy of the aluminum alloy.
- 2) surface chemistry of the adherend.
- 3) prepared oxide layer.
- 4) primer chemistry.
- 5) chemistry of the adhesive system.
- 6) chemistry of the cure cycle.
- 7) synergism of each created interface.

B. Dynamic Environment

- 1) stress.
- 2) humidity and other atmospheric gases.
- 3) temperature.

C. Failure Analysis

- 1) fracture.
- 2) fatigue.
- 3) corrosion.

The appropriate permutations and combinations of A, B, and C should generate a data base capable of advancing our knowledge in the area of life expectancy of adhesively bonded primary structural components of airframes.

SECTION II

INTRODUCTION

Numerous publications on the mechanical properties of metal-to-metal adhesive bonds have shown the effect of the organic resin or primer on bond strength. With the advent of surface instrumentation technology, the effects of the chemical aspects of bonded joints are now being studied (Reference 1). Presently the interface receiving the most attention by surface analysis techniques is the adhesive-oxide interface.

The present paper presents a selection of results obtained from studies designed to generate data from the oxide-metal interface. This particular interface is normally overlooked in the failure analysis of a bonded joint. However, the probability of the cause of structural failure due to bond line corrosion can be high in certain environments. This probability arises from the fact the high strength 2000 and 7000 series aluminum alloys used by the aircraft industry are less corrosion resistant than most of the other aluminum alloys. When the aluminum industry uses these alloys as structural materials they alleviate this problem by cladding (essentially a thin film of commercial grade aluminum placed on the bulk surface). These films are designed to be anodic with respect to the bulk alloy and therefore provide sacrificial protection in corrosive environments. This technique cannot be used when the alloys are adhesively bonded since loss of the sacrificial cladding would mean loss of bond line. The aircraft industry is then required to work with these alloys in the so called "bare" state with the chemical composition as shown in Table 1.

In present day adhesive bonding technology one of the first steps used in the surface preparation of these bare materials is to protect, or passivate, the surface with an anodic thin oxide film. One method is to grow the thin

oxide film electrochemically using phosphoric acid as an electrolyte. It is highly desirable the thin oxide film retain its passivation and adhesive properties while under the influence of stress and environment.

The purpose of this study is to determine what effects the alloying constituents may have on the formation of the anodic oxide film and its passivation properties.

SECTION III

EXPERIMENTAL

1. Surface Preparation

Test materials were cut (25mm x 50mm x 1mm) from commercially available, bare and clad, 2024-T3 and 7075-T6 aluminum. The specimens were acetone wiped, ultrasonically cleaned with carbon tetrachloride for 5 minutes, and then acid pickled. The acid pickle solution consisted of 170 ml of nitric acid, 30 ml of hydrofluoric acid, and distilled water to make one liter. Specimens were submerged for two minutes at room temperature. The effects of these treatments on the alloy surface have been studied previously (Reference 2). The specimens were anodized for 10 minutes at 10 volts using 1.0M phosphoric acid as the electrolyte.

2. Corrosion Solution

Most organic solvents by themselves do not attack aluminum alloys at room temperature; however, a solution containing a mixture of carbon tetrachloride and methanol (Reference 3) is quite reactive at room temperature with aluminum alloys containing copper. Our mixture contained 2 parts (by volume) carbon tetrachloride and one part methanol. Specimens were observed submerged in the corrosion solution using a microscope at 100X.

3. Instrumentation

After removal from the corrosion solution identification of the major elemental species present on the surface or in the corrosion pits was made through the use of Ion Scattering Spectroscopy (ISS), Secondary Ion Mass Spectroscopy (SIMS), Auger Electron Spectroscopy (AES), and Scanning Electron Microscopy (SEM). A description of the first three techniques is reported in Reference 1. Most researchers are familiar with the SEM technique (Reference 4); however, we also have attached to our SEM

system an energy dispersive x-ray detector. With this equipment x-rays can be collected and counted as a function of their energy. In this manner, x-rays from different elements can be collected and the displayed energy spectra will be directly related to the kind of element present in the sample being analyzed.

SECTION IV

RESULTS AND DISCUSSION

We know the chemical properties of the generated anodic oxide film can vary as a function of alloying constituents and chemical surface treatments (Reference 2).

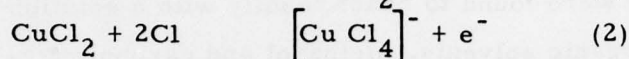
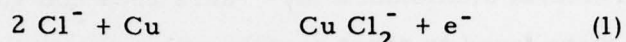
Wood (Reference 5) has reported on the incorporation of alloying elements in the anodic oxide layer of thick ($50\text{ }\mu\text{m}$) films. Our studies (Reference 6) on thin anodic oxide films show the same general trend where alloying elements become part of the growing oxide film. We can see some of these effects in Figure 1 where a HNO_3 -HF treated surface of 2024Al was anodized for 60 seconds in H_3PO_4 . This oxide film is approximately $0.05\text{ }\mu\text{m}$ thick, but the elements fluorine and copper are still detected by SIMS and ISS. Since these chemical inhomogenities can exist throughout the oxide film it is necessary to know if they can be responsible for breakdown of the passive film.

Each specimen was placed individually in the corrosion solution and observed with the use of a binocular microscope. Corrosion was allowed to take place at open circuit potentials. Primary attack on each specimen was recognized at discrete points on the surface by the onset of a stream of bubbles. When the area under observation had initiated 3 to 5 pits the specimen was removed from the solution and rinsed with methanol, then distilled water and dried at 150°F under a heat lamp. What makes this corrosion solution particularly interesting is the fact that pure aluminum, aluminum oxide, and aluminum hydroxide are not readily attacked at room temperature. Therefore, the pitting that occurs will only take place through defects in the anodic oxide film formed on 2024 and 7075. A typical corrosion pit area (Figure 2) is shown in the SEM micrograph. The pit area is then marked and a chemical analysis performed on

them with the surface instrumentation described in Reference 1. It is obvious (Figure 3) that the oxide film is not attacked by the corrosion solution since it continues to support itself across the area that has suffered pit corrosion. Because we allowed pit growth to occur only for a short time most of the corrosion pits were covered with oxide film. This is essentially the same type of pit configuration and growth observed by Barger and Givens (Reference 7); however, their pit growth was initiated by short duration low voltage pulses in comparison to our open circuit potential study.

Figure 4 shows an SEM micrograph of a corrosion pit produced on 2024 aluminum. The pit in this case has no oxide film covering the area. There appear to be small spherical growth products at the bottom of this pit. The electron beam from our Auger spectrometer can be focused into this pit allowing us to obtain an elemental chemical analysis of this area. The data obtained from this pit (Figure 5) shows copper with a large peak to peak intensity with the amplifier sensitivity set at 4X. Some magnesium and manganese are also detected. A pit was formed on a 7075 aluminum specimen and analyzed (Figure 6). The elements copper, zinc, and magnesium were detected. 7075 aluminum contains approximately 5.5% zinc; however, only a small amount is detected in the pit. Auger data obtained outside a pit (Figure 7) was used as a reference point for the elements found within the pit. Elements of primary interest detected outside the pit, are aluminum and oxygen. Figure 8 is an x-ray image of the pit shown in Figure 4. The image depicts the data from the x-ray system set to accept energies for the element copper. The bright images indicate the presence of copper (Reference 8) in the spherical products at the bottom of the pit. Figure 9 shows a mosaic of micrographs. The upper right corner is an SEM electron picture of a pit generated on a 7075 aluminum specimen. The other three micrographs represent x-ray images. The upper left shows the

image obtained from the element chlorine, lower left aluminum, and lower right for copper. Very little chlorine is detected in the pit. We had expected to see larger amounts of chlorine since Vorster (Reference 2) proposed the primary corrosion reaction to be:



Examination of pits on other specimens showed very small amounts of chlorine detected. Our corrosion solution is a 2:1 mixture of CCL_4 : CH_3OH . If the ratio is reversed ($2\text{CH}_3\text{OH}:\text{CCL}_4$) the corrosion rate increases dramatically. The latter solution would represent a large decrease in chloride ion concentration; therefore, it is difficult to understand why the corrosion rate increases if reactions 1 and 2 are the controlling factors. Further work is necessary to better understand the complex chemistry that must be present in this mixture with respect to its corrosive attack on copper containing aluminum alloys.

The clad specimens required a much longer time period (compared to the bare material) in the corrosion solution in order to start pit formation. This was expected since the corrosion solution reacts very slowly with a pure aluminum film* at room temperature. Examination of the pits that eventually occurred showed selective dissolution of certain grain boundaries. An SEM micrograph of one of these pits formed on the surface of 2024 clad aluminum is shown in Figure 10. A similar pit was obtained from a 7075 clad specimen (Figure 11). Neither x-ray energy data or Auger electron spectra detected any of the alloying constituents in the pit. Aluminum and oxygen were the only elements detected. The 7075 clad material was the first to pit. The 2024 clad specimen required a scratch to initiate a pit formation.

* containing <1% copper.

SECTION V

SUMMARY AND CONCLUSIONS

The more important structural aluminum alloys, bare 2024 and 7075, used in the aircraft industry were found to react readily with a solution formed from a mixture of organic solvents, methanol and carbon tetrachloride. This same solution does not react with pure aluminum, aluminum oxide or aluminum hydroxide. The differences in these reaction rates allowed us to use this solution as a corrosion environment for studying anodic oxide film defects formed on these alloys.

A small number of corrosion pits were allowed to grow to approximately 100-micron diameter. This required an 8 to 10 minute time duration. None of the alloying constituents were observed by Auger spectroscopy external to the pits in this time period. Data obtained from within the pits by Auger and SEM-x-ray scans show copper is always present. Magnesium and zinc were detected in the pits of some of the specimens. From this study it is apparent that pit initiation occurs at defects created in the anodic oxide film by the alloying constituents.

In particular we can see that copper present as microparticles or the intermetallic compound CuAl_2 can cause defects in the formed anodic oxide film. These defects are then potential sites for pit corrosion. This chain of events will reduce the long-term service quality of an adhesively bonded structure. This particular interface, the oxide-metal interface, merits more attention from researchers and theorists concerned with metal-to-metal adhesively bonded structures.

SECTION VI

REFERENCES

1. W. L. Baun, N. McDevitt, and J. Solomon, ASTM STP 596, American Society for Testing and Materials, 1976, p. 86.
2. N. McDevitt, W. Baun, and J. Solomon, Air Force Materials Laboratory, Technical Report AFML-TR-75-122, October 1975, Wright-Patterson AFB, Ohio 45433.
3. S. W. Vorster, Corrosion Science 9, 801 (1969).
4. G. W. Kammlott, Surface Science 25, 120 (1971).
5. G. C. Wood, Oxide and Oxide Films, Dekker, N.Y., 1973, p. 223.
6. N. McDevitt and W. Baun, Air Force Materials Laboratory, Technical Report AFML-TR-76-74, June 1976, Wright-Patterson AFB, Ohio 45433.
7. C. B. Barger and R. B. Givens, J. Electrochem. Soc., 124, 1845 (1977).
8. I. Muller and J. Galvella, Corrosion Science, 17, 179 (1977).

TABLE 1
Chemical Composition of 2024 and 7075 Aluminum

Alloy	Cu	Mg	Zn	Fe	Cr	Mn	Si	Ti	Al
2024	3.8-4.9	1.2-1.8	0.25	0.50	0.10	0.3-0.9	0.5		Remainder
7075	1.2-2.0	2.1-2.9	5.1-6.1	0.7	0.1-0.4	0.3	0.5	0.2	Remainder

4He

1.0M H₃PO₄ 60sec.

+ SIMS

ISS

N(E)

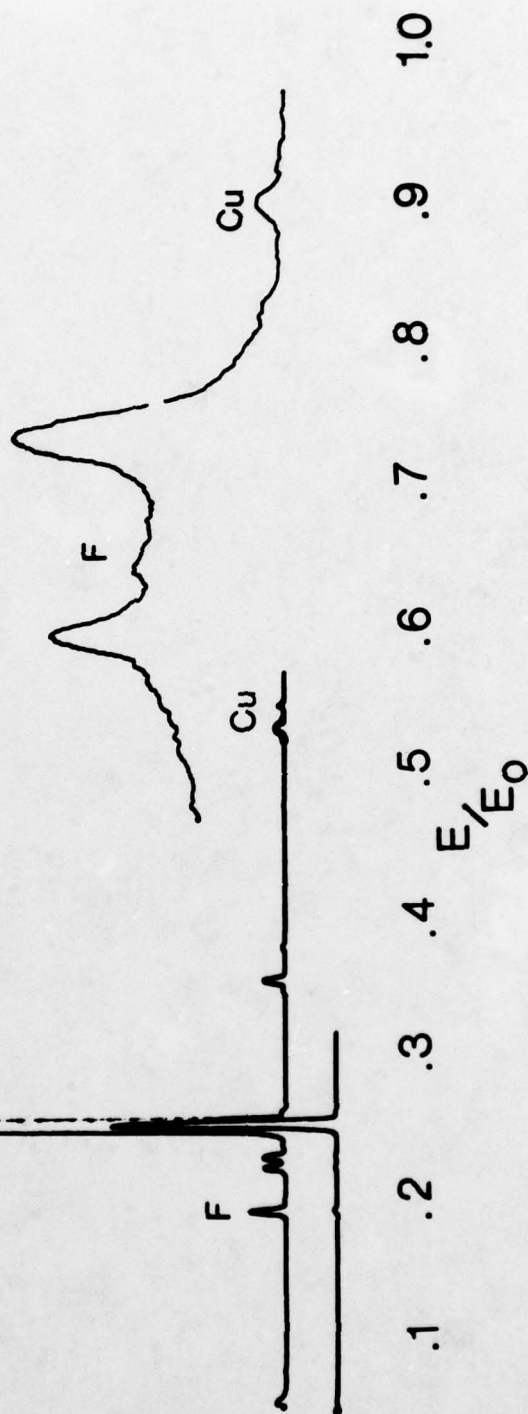


Figure 1. SIMS-ISS Spectrum of Phosphoric Anodized 2024 Specimen



Figure 2. SEM Electron Micrograph of a Typical Pit Corrosion Area

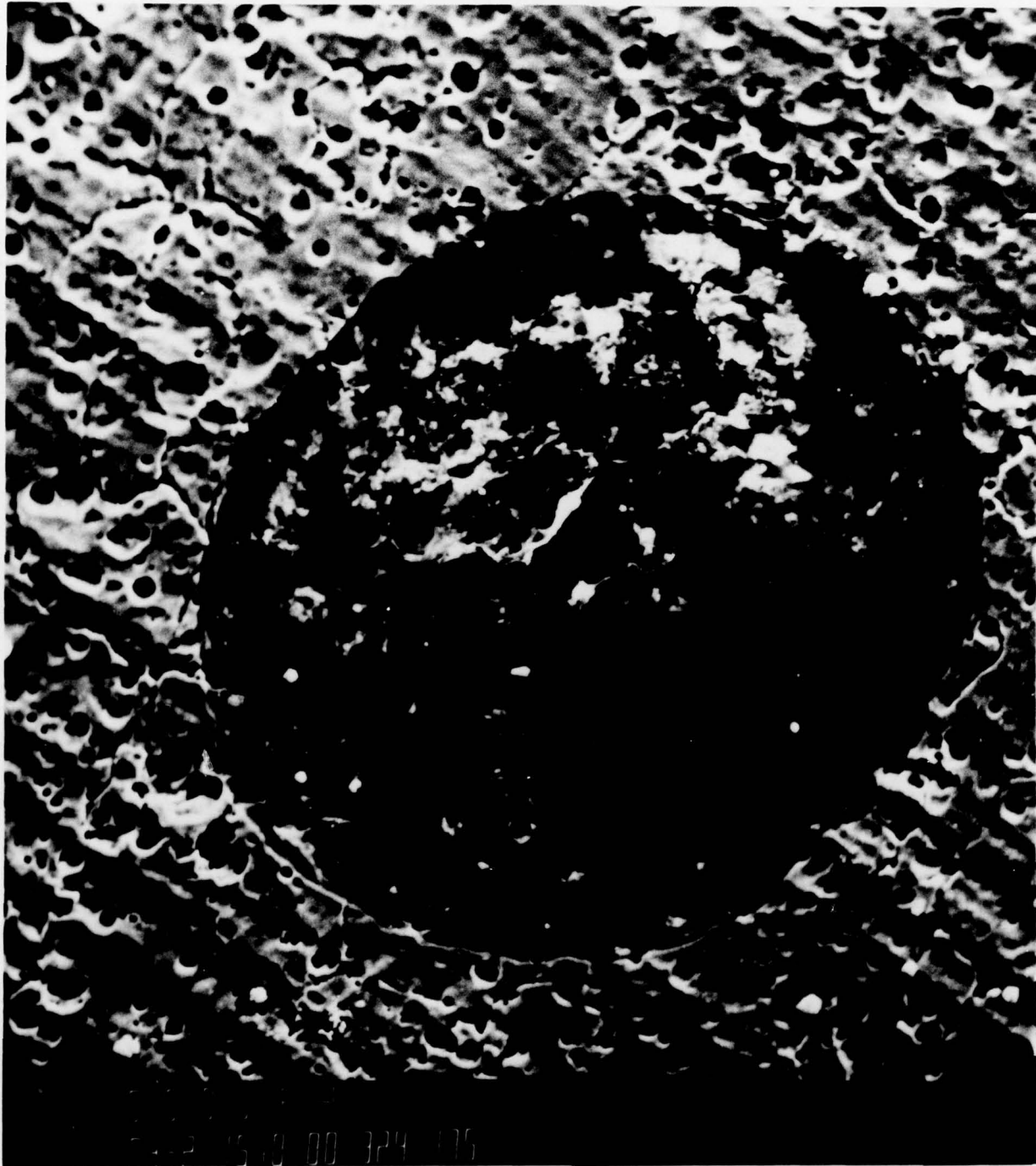


Figure 3. Pit Showing Oxide Film Coverage



Figure 4. SEM Micrograph of a Pit Containing Spherical Growth Products

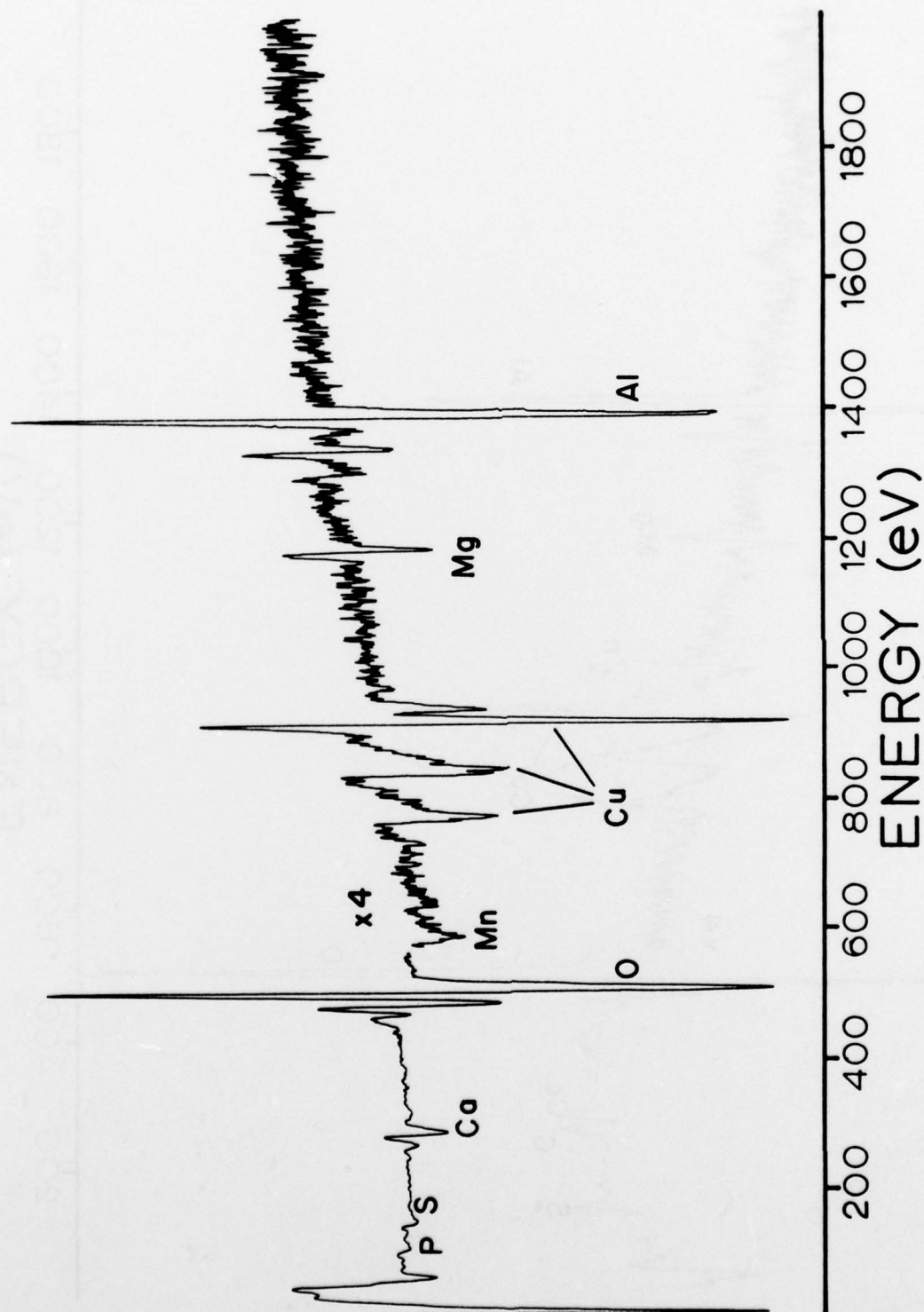


Figure 5. Auger Spectrum of a Pit on a 2024 Aluminum Specimen

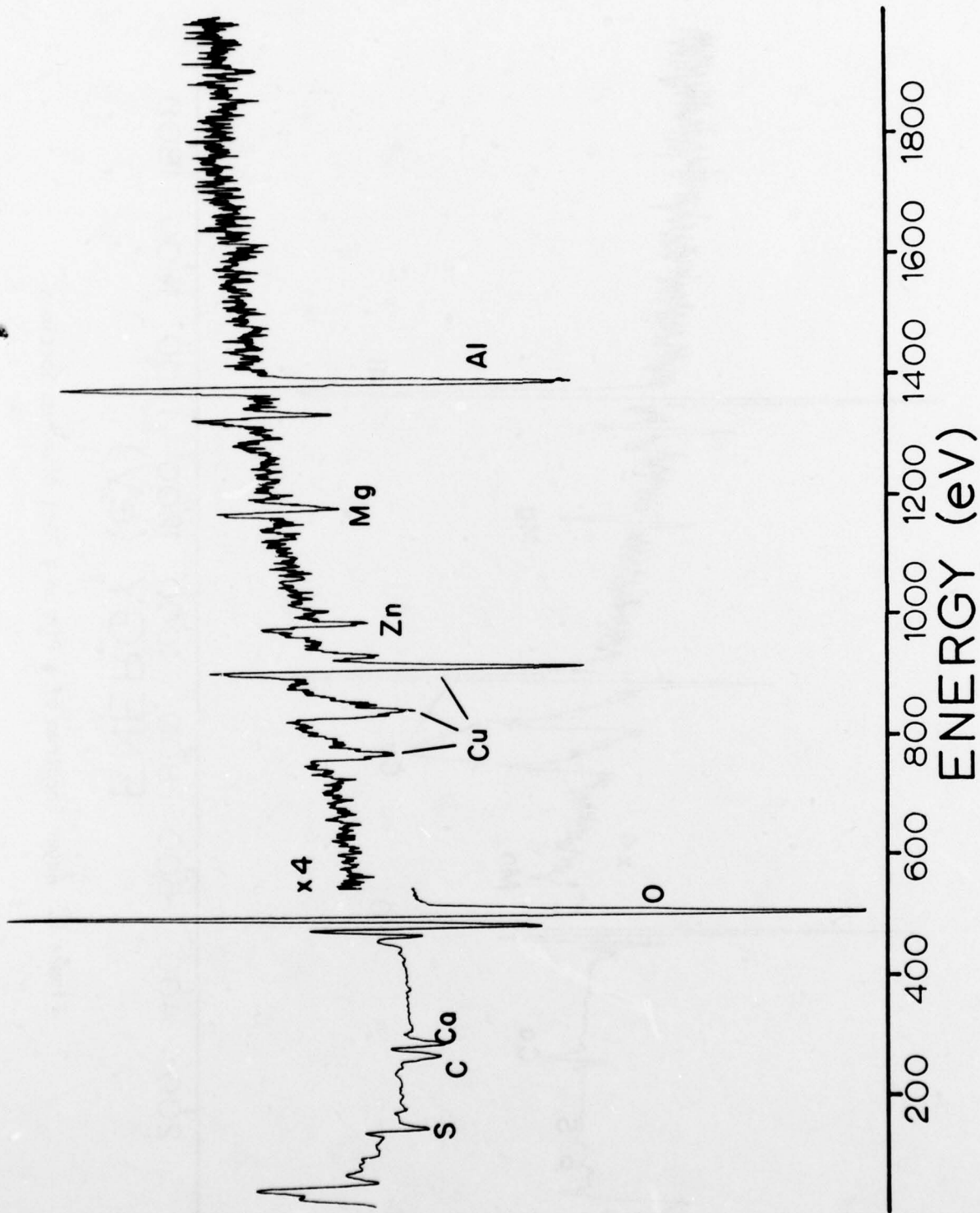


Figure 6. Auger Spectrum of a Pit on a 7075 Aluminum Specimen

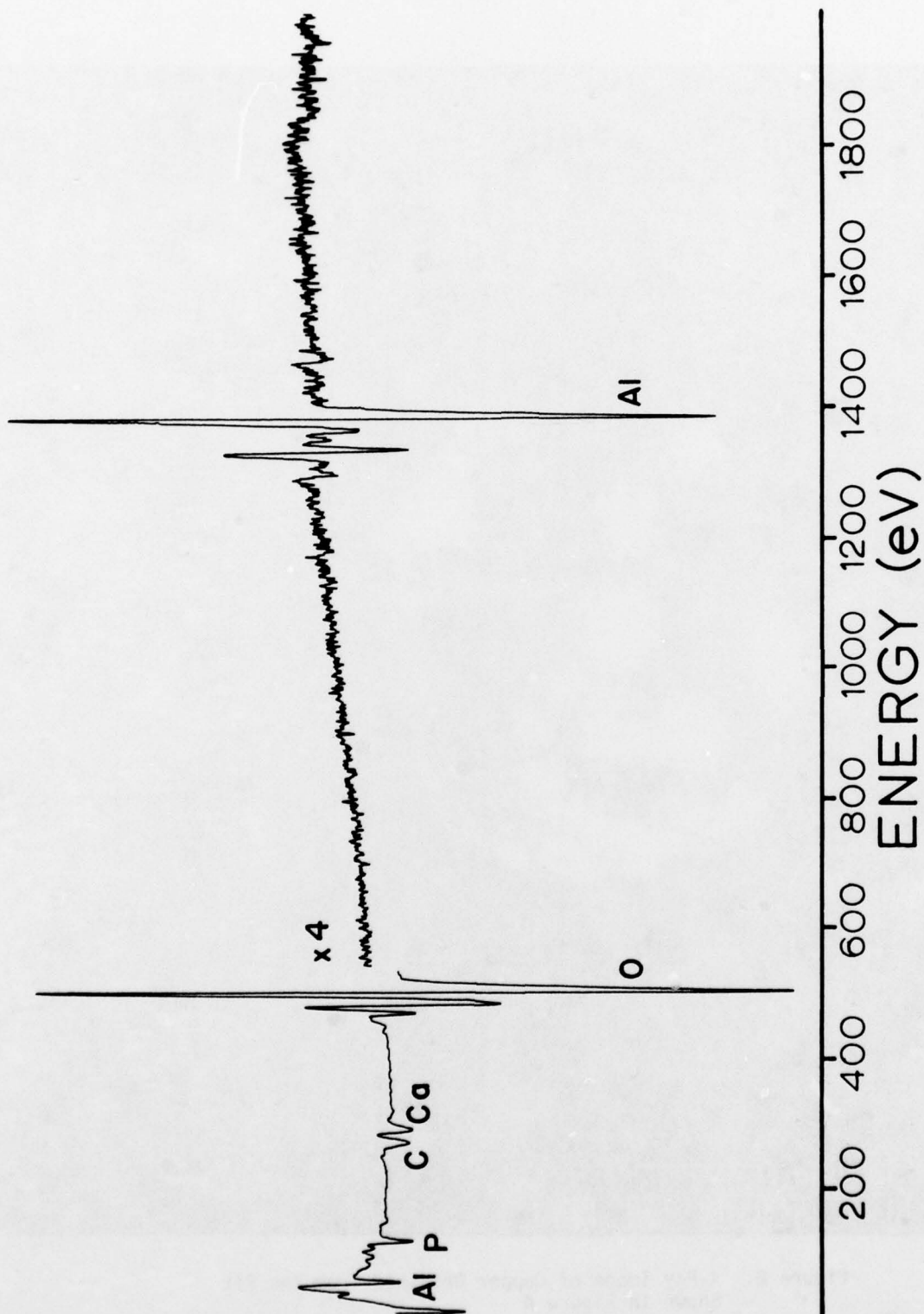


Figure 7. Auger Spectrum from the Surface Area Outside a Pit



Figure 8. X-Ray Image of Copper Obtained from the Pit
Shown in Figure 4

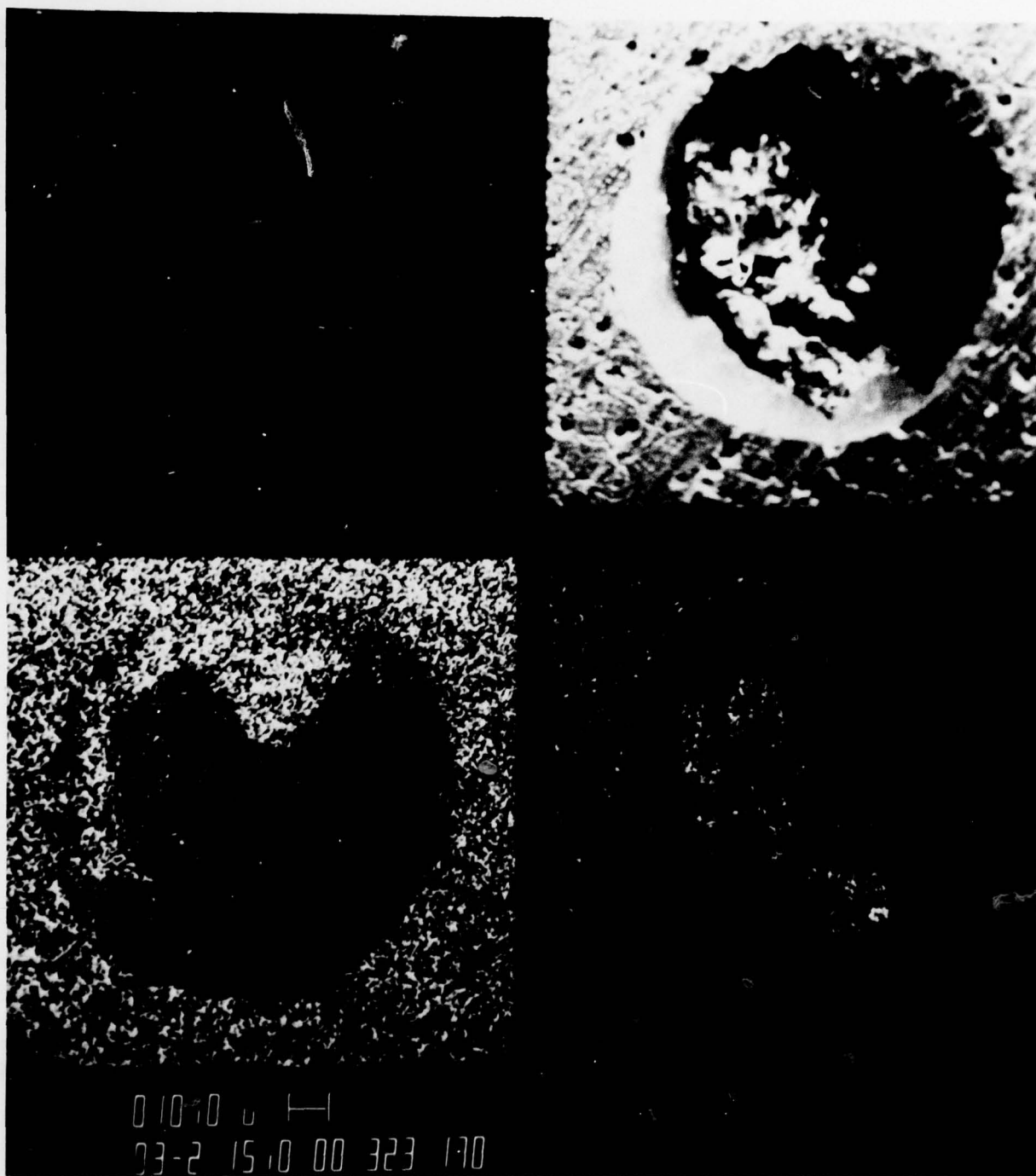


Figure 9. Mosaic of SEM Data. Starting Upper Right Going Clockwise;
SEM Electron Image of 7075 Pit Formation, X-Ray Image of
Copper, X-Ray Image of Aluminum, X-Ray Image of Chlorine



Figure 10. Corrosion Pit Formed on Clad 2024 Showing Preferential Etching of Pit



Figure 11. Corrosion Pit Formed on Clad 7075 Preferential Etching of Pit